IL NUOVO CIMENTO **48 C** (2025) 45
DOI 10.1393/ncc/i2025-25045-x

Colloquia: IWM-EC 2024

Investigations of structure effects in heavy-ion fusion above the Coulomb barrier

I. Lombardo(1)(2), B. Gnoffo(1)(2), D. Dell'Aquila(3)(4), L. Redigolo(1)(2) and F. Porto(1)(5)

(1) *Dipartimento di Fisica e Astronomia "Ettore Majorana", Università degli Studi di Catania Catania, Italy*
(2) *INFN, Sezione di Catania - Catania, Italy*
(3) *Dipartimento di Fisica "Ettore Pancini", Università degli Studi di Napoli "Federico II" Napoli, Italy*
(4) *INFN, Sezione di Napoli - Napoli, Italy*
(5) *INFN, Laboratori Nazionali del Sud - Catania, Italy*

received 26 November 2024

Summary. — We investigated the occurrence of nuclear structure effects in the fusion of heavy ions at above-barrier energies. To unveil the presence of such tiny effects, we developed a semi-classical model based on the modified *Sum-of-Difference* method of nuclear reactions, able to reproduce the gross trend of the whole database available to date. The deviations between the model predictions and the data can be linked, at low bombarding energies, to the occurrence of shell closures; at larger energies, such effects are washed out, while phenomena due to the cluster structure of projectile or target are observed.

1. – Introduction

The interest on the study of heavy-ion fusion can be traced back to the intense campaigns, performed at the end of the '60s, on the route towards the synthesis of super-heavy elements with cyclotrons and LINAC accelerators [1]. As a by-products, several new competing reaction mechanism, different from the fusion-evaporation or fusion-fission scenarios, were reported and investigated, giving the origin to the heavy-ion science as it is usually known today [2]. It became immediately clear that the fusion of heavy ions would give the opportunity of studying nuclear matter under extreme conditions of angular momentum, thermal energy and deformation, allowing to determine the boundaries of existence of excited nuclei [3-5], with interesting implications also in the characterization of the equation of state of nuclear matter [6-10].

Indeed, the complete fusion process itself has been often considered as an interesting cross-over topic between nuclear and soft-state matter: the analogies between dynamics and thermodynamics of interacting liquid drops and fusing heavy ions are so striking that several scaling laws and dynamical effects are similar in both the contexts [11, 12].

In the nuclear case, indeed, some specific aspects affect the dynamics of heavy-ion fusion. For example, the shell structure of nuclei has a strong influence on the fusion dynamics in the sub-barrier regime [13]. Furthermore, in the nuclear case, the trend of the excitation function of complete fusion cross-section shows three separate regimes (called Regions, see, *e.g.*, [14-16]), characterizing respectively the slightly over-barrier region (Region I, where the reaction flux is almost fully exhausted by complete fusion), the region were other reaction mechanisms are in strong competition with fusion (Region II), where deep inelastic and incomplete fusion events are present), and the intermediate energy regime (Region III), where complete fusion cross-section quickly drops toward zero, being fully replaced by more complex phenomena (as multi-fragment emission [7, 17,18]). The presence of a so rich phenomenological scenario makes it particularly difficult to extract the (tiny) effects due to nuclear structure aspects (shell closures, deformations, clustering, etc.) of the colliding partners [19, 20].

For this reason, we decided to develop a new phenomenological model, based on the paradigm of the modified Sum-of-Difference (mSOD) method of nuclear reactions [21], able to describe the gross trend of a huge experimental database of about 5000 experimental cross-section points, for reaction partners in the region $12 \leq A \leq 180$, and total masses smaller than $A \simeq 220$. On the average, more than 70% of experimental cross-section data deviates for less than 20% with respect to the present model predictions, making the model a good instrument to inspect fusion suppression or enhancements due to specific nuclear structure parameters of the entrance channel [22].

After a short description of the model implementation and interpolating power, we describe in sect. **3** the effects due to the shell closure and the Q_α disintegration threshold in the complete fusion cross-section respectively in the low- (Region I) and high-energy (Regions II and III) regimes.

2. – Complete fusion and the mSOD approach

The reaction cross-section in the mSOD approach can be semi-classically expressed as [21, 23] $\sigma_r = 2\pi \int_{\theta_a}^{\pi} \{\sigma_R(\theta) - \sigma_{el}(\theta)\} \sin\theta \mathrm{d}\theta$, being $\sigma_R(\theta)$ and $\sigma_{el}(\theta)$ the Rutherford and elastic differential cross-section, respectively, and θ is the scattering angle in the center of mass frame. In this frame, when $\theta < \theta_a$, we assume that the absorption process ceases [21, 24]. Since the fusion cross-section σ_f is always smaller than σ_R, there will exist an angle $\theta_f \geq \theta_a$ for which $\sigma_f = 2\pi \int_{\theta_f}^{\pi} \{\sigma_R(\theta) - \sigma_{el}(\theta)\} \sin\theta \mathrm{d}\theta$. In the elastic scattering of heavy ions, strong absorption effects allow the simplification $\sigma_f \approx 2\pi \int_{\theta_f}^{\pi} \sigma_R(\theta) \sin\theta \mathrm{d}\theta$. Solving the integral, we will find

$$\sigma_f = \pi \left(\frac{\eta}{k}\right)^2 \cot^2 \frac{\theta_f}{2} = \frac{\pi}{k^2}(kD)^2 \left(1 - \frac{2\eta}{kD}\right), \tag{1}$$

being η the Sommerfeld parameter, k the wave number, and D the distance of closest approach, that is connected to θ_f. D can be factorized as $D = d(\sqrt[3]{A_1} + \sqrt[3]{A_2})$, being d a parameter dependent on the energy and other structure characteristics of the colliding system. In this way we will get

$$\sigma_f = \frac{\pi}{k^2}(\sqrt[3]{A_1} + \sqrt[3]{A_2})^2 (kd)^2 \left(1 - \frac{2\eta}{\sqrt[3]{A_1} + \sqrt[3]{A_2}} \frac{1}{kd}\right). \tag{2}$$

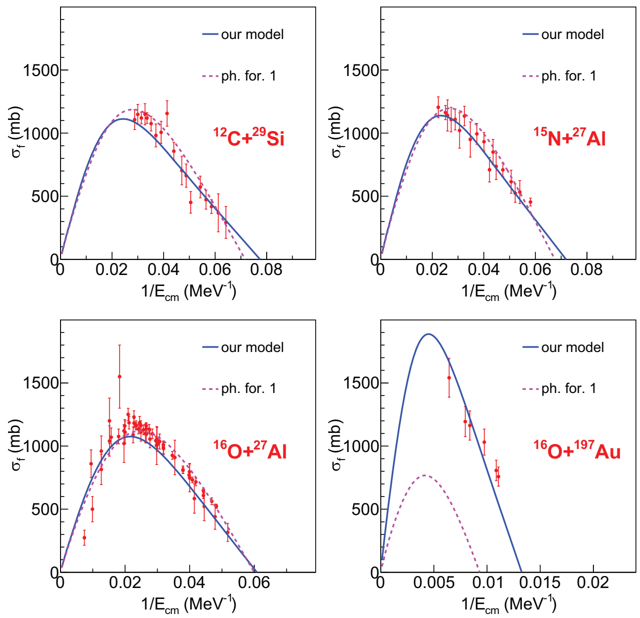

Fig. 1. – Examples of complete fusion cross-section data (dots) reproduced with the presently discussed model based on the mSOD method (solid lines), and compared with model predictions of ref. [23] (dashed lines).

If we define $F(\varepsilon) = \frac{kd}{A_{tot}}$ eq. (2) transforms as

$$\sigma_f = \frac{C_1}{E} F(\varepsilon) \left[C_2 F(\varepsilon) - \frac{C_3}{\sqrt{E}} \right]. \tag{3}$$

The constants C_1, C_2, C_3 depend on the masses and charges of the entrance channel; their expressions are given explicitly in [22].

Following this approach, we transformed all the experimental points of the fusion database in $(kd)_{exp}$ values. We found a series of interesting scaling laws as a function of the total mass of the fused system, the entrance channel mass asymmetry and neutron excess and the penetrability of the Coulomb barrier, discussed in details in ref. [22], that allows to simply parameterize the $\frac{kd}{A_{tot}}$ value, and consequently the fusion cross-section as follows:

$$\frac{kd}{A_{tot}} = F(\varepsilon, \Delta, n) = a \cdot f_A(\Delta, n) \cdot g_v(\varepsilon) \cdot h_C(\varepsilon), \tag{4}$$

being a an overall constant, $f_A(\Delta, n)$ a function describing the effects of mass and isospin asymmetries, $g_v(\varepsilon)$ describing the effects of friction forces in the relative motion energy damping and $h_C(\varepsilon)$ a correction term useful to describe the trend of data close to the Coulomb barrier. The explicit expression of such functions, and their physical meaning and interpretations, are discussed in details in ref. [22]. It is worth noting that the proposed model has only four free parameters, adjusted simultaneously to the very broad database of ref. [25]. The predictive capabilities of our model were tested by using the 70% of data (randomly chosen) to derive the model, and the remaining 30% of data as a benchmark for extrapolations. On the average, more than 70% of experimental points used to test the model deviate for less than 20% with respect to the model predictions. If compared to previous state-of-the-art models of refs. [23] and [26], an improved description of the entire dataset is observed, especially for heavier systems (see ref. [22] for further details).

Examples of complete fusion cross-section data reproduced by the present model are reported in fig. 1, for typical collision systems in the $A_{tot} \approx 40$–200 range. Blue solid lines are the results of the phenomenological model derived in this work, compared with similar predictions derived from ref. [23].

3. – Structure effects in heavy-ion complete fusion

As discussed in the introduction, nuclear structure effects can influence over-barrier fusion: for example, shell closures can affect the saddle point and/or the density distributions [27], while α clustering can led to strong competitions between reaction mechanisms very different from fusion [28,29]. In this investigation, we sorted the experimental data into two groups on the basis of the relative velocity of the reaction partners (see, *e.g.*, [26,30]): data with $v_{rel} \leq 0.06c$ would correspond mainly to Region I, while Region II+III are selected with the boundary $v_{rel} > 0.065c$.

We then calculate the *average* deviation between data and model predictions, defined as $\langle \delta_n \rangle = \frac{\Sigma \delta_{n,i}}{N}$, being $\delta_{n,i}$ the deviation $\left(\frac{\sigma_{exp} - \sigma_{mod}}{\sigma_{exp}}\right)$ of the i-th cross-section data related

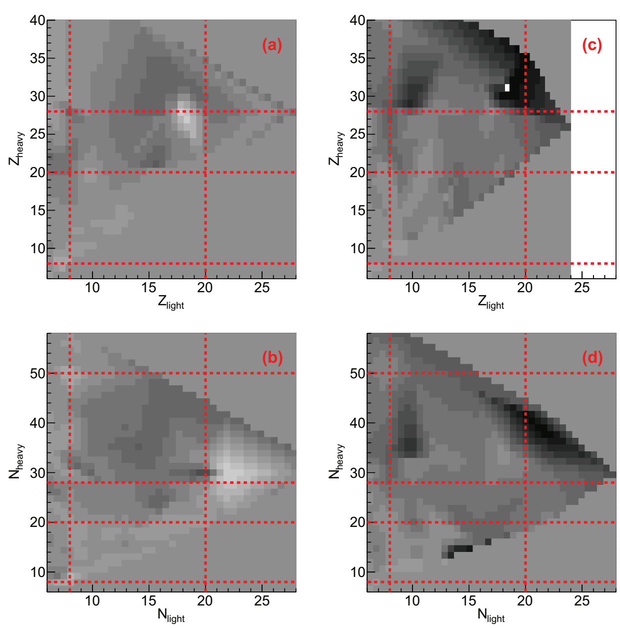

Fig. 2. – Distributions of the average deviations between data and model predictions, as a function of Z (panels (a) and (c)) or N (panels (b) and (d)) of the colliding ions. Darker grays are associated to negative deviations, while lighter grays indicate positive deviations. Dashed lines indicate shell closures. Panels (a) and (b): $v_{rel} < 0.06c$; panels (c) and (d): $v_{rel} > 0.065c$.

to a collision system in a given selection, and N the number of points. In fig. 2, we show average deviation maps as a function of Z (panels (a), (c)) and N (panels (b), (d)) of the colliding ions, for Region I (panels (a), (b)) and Regions II+III (panels (c), (d)) data. The gray color scales indicate positive (lighter grays) or negative (darker grays) average deviation values.

The map of deviations shows sizable positive deviations for colliding partners near a shell closure. This effect is particularly pronounced for colliding nuclei slightly lower than the $Z = 20{,}28$ shell closure; a correspondent bump is seen in panel (b) just above the $N = 20{,}28$ shell closure. Smaller positive deviations are seen also close to other shell closures (*e.g.*, $Z = 8{,}8$ and $N = 8{,}8$ and 8,50); these findings, indicating an enhancement of the fusion cross-section close to a shell closure, are in qualitative agreement with the findings of ref. [27]. Region II+III data, shown in fig. 2(c), (d), indicates a complete disappearance of such effects, due to the washing out of shell effects at larger excitation energies in the fused system.

In fig. 2(c), (d) we can recognize also a localized region in which our model over-predicts the cross-section: this occurs at $Z_{light,heavy} \approx [9\text{–}10; 29\text{–}35]$ and $N_{light,heavy} \approx [9\text{–}10; 32\text{–}40]$, without counterpart in the Region I data. A simple interpretation of this effect could be due to very small α decay thresholds observed for nuclei in the $A \approx 20$ region [31]; such nuclei can be more inclined to trigger α-transfer, incomplete fusion or pre-equilibrium α events that, at high energies, are in competition with complete fusion events [29].

4. – Conclusions

In this work we discussed the development of a semi-classical model based on the modified Sum-of-Difference method, to describe in an effective way a large body of complete fusion cross-section data with just four free parameters. The excellent description of data allows to investigate fine deviations between experimental data and model predictions. A topological analysis of the deviation maps indicates the possible influence of shell effects in the fusion cross-section for above-barrier collisions, that are washed out at larger relative energies. A suppression of complete fusion events at large energies is observed when using colliding partners with low α threshold, signaling the strong competition between fully damped reaction mechanisms and partial momentum transfer phenomena triggered by the α cluster structure of reacting nuclei.

REFERENCES

[1] Bass R., *Phys. Rev. Lett.*, **39** (1977) 265.
[2] Bromley D. A., *Treatise on Heavy-Ion Science*, Vol. **2** (Plenum Press) 1984.
[3] Lombardo I. *et al.*, *Nucl. Phys. A*, **834** (2010) 458c.
[4] Lombardo I. *et al.*, *Phys. Rev. C*, **82** (2010) 014608.
[5] Pirrone S. *et al.*, *Eur. Phys. J. A*, **55** (2019) 22.
[6] Amorini F. *et al.*, *Phys. Rev. Lett.*, **102** (2009) 112701.
[7] De Filippo E. *et al.*, *Acta Phys. Pol. B*, **40** (2009) 1199.
[8] Cardella G. *et al.*, *Phys. Rev. C*, **85** (2012) 064609.
[9] Borderie B. *et al.*, *Phys. Lett. B*, **782** (2018) 291.
[10] Baldesi L. *et al.*, *Phys. Rev. C*, **109** (2024) 064618.
[11] Bremond N., Thiam A. and Bibette J., *Phys. Rev. Lett.*, **100** (2008) 024501.
[12] Akella V. S. and Gidituri H., *Chem. Phys. Lett.*, **758** (2020) 137917.

[13] Denisov V. Y., *Phys. Rev. C*, **89** (2014) 044604.
[14] Lee S. M., Matsuse T. and Arima A., *Phys. Rev. Lett.*, **45** (1980) 165.
[15] Arena N. *et al.*, *Phys. Rev. C*, **44** (1991) 1947.
[16] Pirrone S. *et al.*, *Phys. Rev. C*, **64** (2001) 024610.
[17] Frosin C. *et al.*, *Phys. Rev. C*, **107** (2023) 044614.
[18] Ciampi C. *et al.*, *Phys. Rev. C*, **108** (2023) 054611.
[19] Dell'Aquila D. *et al.*, *J. Phys.: Conf. Ser.*, **2619** (2023) 012004.
[20] Dell'Aquila D., Gnoffo B., Lombardo I. and Porto F., *Phys. Lett. B*, **837** (2023) 137642.
[21] Giordano R. *et al.*, *Nuovo Cimento A*, **61** (1981) 182.
[22] Dell'Aquila D., Gnoffo B., Lombardo I., Porto F. and Russo M., *J. Phys. G.: Nucl. Part. Phys.*, **50** (2023) 015101.
[23] Porto F. and Sambataro S., *Nuovo Cimento*, **83** (1984) 339.
[24] Marty C., *Z. Phys. A*, **322** (1985) 499.
[25] Zagrebaev V. I., Denikin A. S., Karpov A. V., Alekseev A. P., Naumenko M. A., Rachkov V. A., Samarin V. V. and Saiko V. V., *NRV web knowledge base on low-energy nuclear physics* (1999) `http://nrv.jinr.ru/`.
[26] Kailas S. and Gupta S. K., *Z. Phys. A*, **302** (1981) 355.
[27] Sing V. *et al.*, *Phys. Rev. C*, **104** (2021) L041601.
[28] Morelli L. *et al.*, *Phys. Rev. C*, **99** (2019) 054610.
[29] Asnain M. S. *et al.*, *Phys. Rev. C*, **104** (2021) 034616.
[30] Fonte R. and Oeschler H., *Phys. Lett. B*, **96** (1980) 265.
[31] Redigolo L. *et al.*, *J. Phys. G: Nucl. Part. Phys.*, **51** (2024) 075106.